Short Papers

A Broad-Band Temperature-Controlled System for the Study of Cellular Bioeffects of Microwaves

A. RIAZI, D. W. HILL, M. J. HAGMANN, MEMBER, IEEE, O. P. GANDHI, FELLOW, IEEE, AND J. A. D'ANDREA, MEMBER, IEEE

Abstract—**A system for the study of cellular bioeffects in the frequency range of 38 to 48 GHz and 65 to 75 GHz is described. High coupling efficiency (greater than 99 percent) provides a method for determining the energy absorption by the samples. An aqueous test medium was pumped through tapered waveguide sample holders. Temperature differences as low as ± 0.01°C were measured using pairs of thermocouples. Compensatory electrical heating of the control sample holders was employed for reduction of temperature differences.**

I. Introduction

Frequency-specific biological effects of millimeter wave irradiation have previously been reported for the 65–75 GHz [1] and 38–48 GHz [2], [3] bands. These pertain to purported changes in growth rate of *Escherichia coli* [1] and yeast cells [2] and alterations in metabolic activities, proliferation, and mitosis in animal cells in culture [3].

One of the reports [3] does not describe the microwave exposure system used for the experiments, and the systems described by the other reports [1], [2] appear to have several drawbacks. For example, Grundler and Keilmann [2] employed a dielectric antenna to irradiate yeast suspensions. We believe that there may have been an uncertain pattern of energy deposition in the sample and an inaccurate specification of the total dose received by the sample. It was not possible to use simultaneous control samples, and there was no provision for control of sample temperatures. The system of Berteaud *et al.* [1] included a horn antenna to irradiate samples in a petri dish. Energy coupling to the samples was low and frequency dependent; thus it was difficult to quantify the data.

An exposure system designed for the study of cellular bioeffects of microwaves must allow precise measurement and control of the sample temperature, frequency of radiation, and the electromagnetic energy absorbed by the sample. Irradiated and control samples must be tested simultaneously. High energy coupling efficiency is particularly important at millimeter wavelengths in order that relatively inexpensive low-power sources may be used. It is also desirable that the system be simple to operate.

The exposure system described in this paper meets the essential requirements and is being used for several studies on cell suspensions. A limitation of the system is that it exposes biological systems during their time of transit past the waveguide. This, however, is the case with the previous systems [1] where, on account of stirring, the individual cells are exposed only when they are within a depth on the order of 0.3–0.5 mm (corresponding to a skin depth) of the irradiated surface.

Manuscript received April 6, 1982; revised May 24, 1982. This work was supported by the U.S. Air Force School of Aerospace Medicine, Brooks Air Force Base, TX 78235, under Contract F33615-79-C-0614.

A. Riazi, M. J. Hagmann, O. P. Gandhi, and J. A. D'Andrea are with the Department of Electrical Engineering, University of Utah, Salt Lake City, Utah 84112.

D. W. Hill is with the Department of Cellular, Viral and Molecular Biology, University of Utah, Salt Lake City, UT 84112.

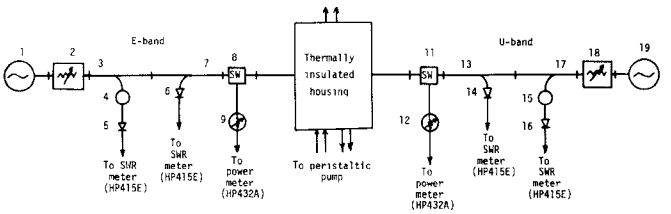

1. Klystron (OKI 70V11A)
2. Precision attenuator (FXR, type M164A)
3 and 7. 10 dB directional coupler (Narda)
4. Frequency meter (Hitachi model S2270)
5 and 6. Diode
8. Waveguide switch (Hughes)
9. Thermistor mount (Hughes model 44895H)
11. Waveguide switch (Hughes)
12. Thermistor mount (Hughes model 44892H)
13 and 17. 10 dB directional coupler (Narda)
14 and 16. Diode
15. Frequency meter (Hitachi model F2210)
18. Precision attenuator (Hitachi model F1513)
19. Klystron (OKI model 45V12 or OKI model 40V12)

Fig. 1. Schematic of irradiation system.

II. System Description

A schematic of the irradiation system is shown in Fig. 1. Simultaneous testing at frequencies in the *E*-band (from 65 to 75 GHz) and in the *U*-band (from 38 to 48 GHz) is possible. A waveguide switch is used in both circuits to allow for the accurate measurement of incident power levels with thermistor detectors. The coupling of microwave to the samples is near-perfect, hence the power absorbed by the sample is equivalent to the power measured by the thermistor mounts. Continuous monitoring of both incident and reflected power is done with SWR meters connected to the broad-band diodes attached to directional couplers in the two circuits.

The thermally insulated housing is illustrated in Fig. 2. The copper base plate of the housing has a temperature set with a proportional temperature controller. Irradiation and dummy (control) waveguides are fastened to the base plate to minimize the temperature differences of the samples. The housing has an aluminum cover and contains Styrofoam insulation to reduce transfer of heat from the base plate. Copper-constant thermocouples are used to monitor fluid temperatures at input and output of each sample holder. A multichannel switch is used to connect various opposing pairs of thermocouples for monitoring the following temperature differences:

1) output of irradiated versus input of irradiated;
2) output of control versus input of control;
3) output of irradiated versus output of control; and
4) input of irradiated versus input of control.

A nichrome heater is fastened on the outside of the glass of each control sample holder so that electrical heating may be used to reduce the observed temperature differences caused by deposition of microwave energy.

Fig. 3 is a diagram of the sample holders. The waveguide is cut along a plane perpendicular to the narrow walls of the waveguide. A glass tube having a rectangular cross section is attached to cover the resulting opening in the waveguide. The edges of the glass tubing are covered with silver paint to prevent microwave leakage. (Since the dimensions of the two sample holders are

0018-9480/82/1100-1996$00.75 ©1982 IEEE

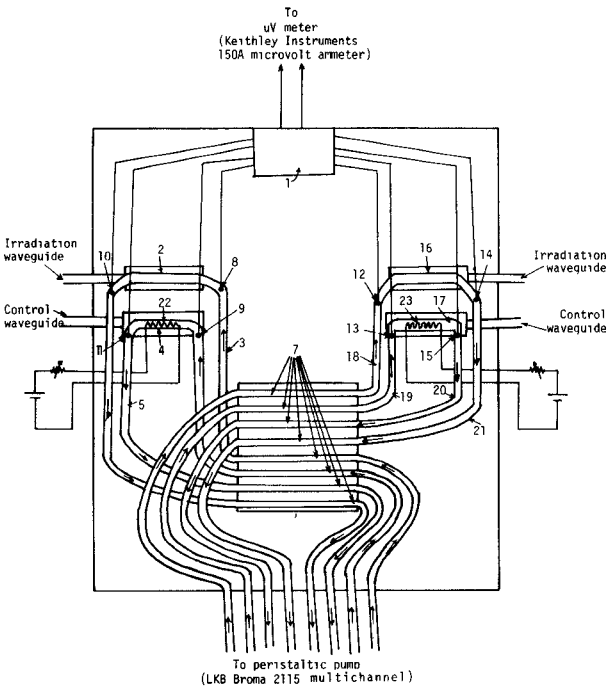

1. Multichannel switch
2 and 16. Sample holder mounted on irradiation waveguide
3, 5, 18, 19, 20, and 21. Rubber tubing (I.D. = 1.3 mm)
4 and 17. Sample holder mounted on control waveguide
7. Metallic tubing mounted on metallic blocks with heat sink paste
8-15. Position of thermocouples
22 and 23. Nichrome wire

Fig. 2. Diagram of insulating housing.

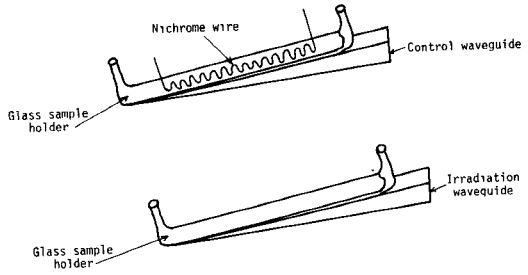

Fig. 3. Sample holders for control (upper drawing) and for irradiation channels (lower drawing)

selected to be at least 3.8 times the skin depth at the respective frequencies, negligible energy leaks through the sides of the sample holders; nevertheless, silver paint is used to further contain the fields within the samples.) The tapered design of the sample holders is used to improve coupling of microwave energy to the sample.

III. System Characteristics

A. Characteristics of the Microwave Circuits

Following a 30-min warm-up period, the microwave power and frequency are constant to within ± 2 percent and ± 0.025 GHz, respectively, (throughout several hours of operation). The sample holders allow a coupling efficiency of greater than 99 percent over all usuable frequencies.

B. Thermal Characteristics of the System

Fig. 4 illustrates the temperature difference between output ports of the irradiated and control sample holders as a function of time for three values of microwave power at 70.5 GHz (pumping rate was 3.78 ml/min).

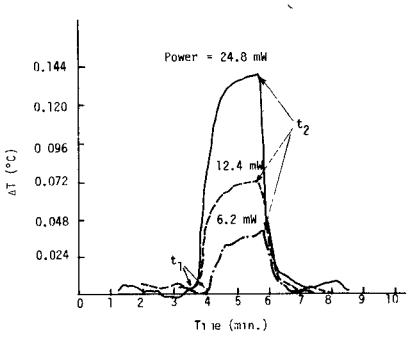

t_1 → Time microwave was applied
t_2 → Time microwave was turned off
Frequency = 70.5 GHz
Flow rate = 3.78 ml/min

Fig. 4. Temperature difference between output ports of control and irradiated sample holders for various microwave powers.

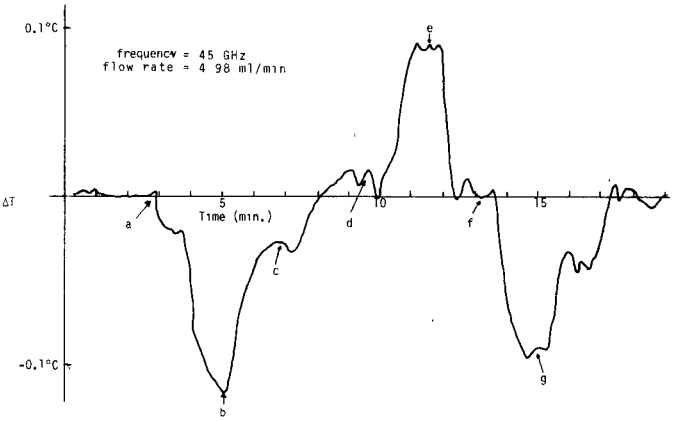

Fig. 5. Temperature difference between output of irradiated and control. *a*: microwave applied (23 mW); *b*: electric heat applied; *c*: electric heat increased; *d*: microwave turned off; *e*: microwave turned on again; *f*: electric heater turned off; *g*: microwave turned off.

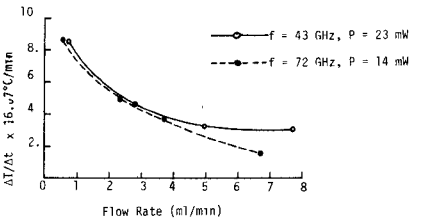

Fig. 6. The heating rate as a function of flow rate.

Fig. 5 records the temperature difference between output ports of the irradiated and control sample holders as a function of time. At time *a*, 23 mW of microwave power was applied to the irradiated samples; at time *b*, electric heat was applied to control samples; at *c*, electric heat was increased; at *d*, microwave power was turned off; at *e*, microwave was turned on again; at *f*, electric heat was turned off; and at *g*, microwave was turned off. The figure illustrates that the nichrome heater may be used to compensate for electric heating of control samples.

Fig. 6 illustrates the effect of flow rate on heating rate. The theoretical rate of heating, neglecting heat transfer from the fluid in the sample holder, is given by $\Delta T/\Delta t = P/4.186$ mc, where P is the applied microwave power in watts (14×10^{-3} W for *E*-band and 23×10^{-3} W for *U*-band), m is the mass of fluid in the sample holder in grams (0.103 *g* for *E*-band and 0.269 *g* for

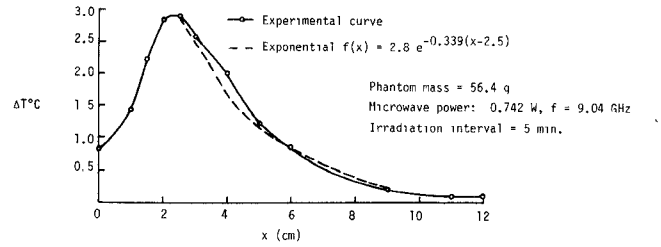

Fig. 7. Heating distribution along the central axis of sample holder.

U-band), and *c* is the specific heat of the sample (1 cal/g °C for water). Hence, neglecting heat loss by the fluid, the expected rate of heating is 0.0325 °C/s for *E*-band and 0.0204 °C/s for *U*-band. Initial values of the heating rate in Fig. 6 are seen to decrease with increasing flow rate as heat transfer from the sample holder is increased.

To determine the distribution of microwave energy deposition within the sample holders, we have measured local heating within a scaled sample holder at *X*-band. Convective heat transfer was eliminated by using phantom compositions with appropriately scaled dielectric constant and conductivity [4] in place of water. Fig. 7 shows the temperature profile along the central axis *x* of the scaled sample holder. The decrease in energy deposition with axial distance is approximately exponential as theoretically expected.

IV. Conclusions

A broad-band temperature-controlled system for the study of cellular bioeffects of microwaves has been developed. The system coupling efficiency is greater than 99 percent over the frequencies used, and it is simple to operate.

Opposing thermocouples allow the measurement of temperature differences as small as ± 0.01°C. Compensatory heating of the control sample holders suggests that temperature differences over the course of 30 min of exposure can be kept within ± 0.02°C by use of appropriate feedback control circuits. This degree of accuracy is desirable in the study of microwave bioeffects.

To date, this system has been successfully employed in investigation of possible effects of microwaves on induction of Lambda phage in lysogenic strains of *E. coli* (both wild type [5] and a temperature-sensitive mutant) and back mutation of *Salmonella Typhimurium* cells (strain types TA1535 and TA1538) possessing His$^-$ mutations.

Our system has been designed for use at *U*- and *E*-bands, but it can be readily scaled for use at other waveguide bands.

References

[1] A. J. Berteaud, M. Dardalhon, N. Rebeyrotte, and D. Averbeck, "Effects of electromagnetic radiation of millimeter wavelength on bacterial growth," (in French), *C. R Acad.* (D), Paris, vol. 281, 1975.

[2] W. Grundler and F. Keilman, "Nonthermal effects of millimeter microwaves on yeast growth," *Z. Naturforsch*, vol. 33C (1/2), pp. 15–22, 1978.

[3] N. P. Zabyubouskaya and R. L. Kiselev, "Biological oxidation in cells under the influence of radiowaves in the millimeter range," *Tritologia I. Genetika*, vol. 3, 1978, pp. 232–235; U.S. Joint Publication Research Service Rep. JPRS L/7957.

[4] A. Y. Cheung and D. W. Koopman, "Experimental development of simulated biomaterials for dosimetry studies of hazardous microwave radiation," *IEEE Trans. Microwave Theory Tech.*, vol. MTT-24, pp. 669–673, 1976.

[5] D. W. Hill, A. Riazi, O. P. Gandhi, and M. J. Hagmann, "Effects of *U*- and *E*-band millimeter wave irradiation on induction of lambda phage," *Abstracts of Third Annual Conf. of Bioelectromagnetic Society*, (Washington, DC), Aug. 9–12, 1981, p. 17.

Microwave Diffraction Tomography for Biomedical Applications

J. CH. BOLOMEY, A. IZADNEGAHDAR, L. JOFRE, CH. PICHOT, G. PERONNET, AND M. SOLAIMANI

***Abstract*—This short paper points out the realizability of a method suitable for quasi real-time coherent microwave tomography for biomedical applications.**

I. Introduction

Recent experiments have shown the potential interest of active microwave imaging in biomedical applications [1]–[3]. The success of this new technique is largely dependent on the practical possibility of realizing rapid tomographic reconstruction and at low cost. This paper describes a promising method providing a good compromise between rapidity and cost. Its salient points consist in the principles of both the equipments and algorithms used in view of tomographic reconstruction. Firstly, the electromagnetic field probing is very fast and inexpensive compared to other conventional solutions using electronic or mechanical scanning. Secondly, instead of assuming straight line propagation, as is usually done in computerized tomography [3], diffraction effects are taken into account.

II. Tomographic Algorithm

The tomographic process is achieved by simulating a focusing system characterized by small field depth and a variable focal length as depicted in Fig. 1. The focusing system transforms the divergent wavefront scattered by the organ under test into a convergent one from which an image can be derived. For a given focal length, the image corresponds to a thin organ slice. The cross section of the organ can be deduced from the different slices obtained by changing the focal length. The slice images are calculated from the field distribution measured in the aperture plane of the simulated focusing system. The reconstruction depends on the illumination and on the observation: the field at the organ location must be as uniform as possible and the length of the observation domain must be $2D + d$ where d is the length of the organ slice in the direction parallel to the observation line and D is the distance between the observation line and the slice.

The organ is seen by its equivalent currents $\boldsymbol{J}$ given by

$$\boldsymbol{J}(x,y) = \left[K^2(x,y) - K_m^2\right]\boldsymbol{E}_t(x,y) \tag{1}$$

where $\boldsymbol{E}_t(x,t)$ and $K(x,y)$ are, respectively, the total field and the wavenumber inside the organ, and K_m is the wavenumber of the homogeneous surrounding medium.

The equivalent currents J are responsible for the scattered field $\boldsymbol{E}_S$. For instance, in the simple case in cylindrical objects illuminated by a plane wave, the electric field of which is parallel to the cylinder Z-axis, the scattered field is related to the equivalent current by

$$\boldsymbol{E}_S(x,y) = \int_S \boldsymbol{J}(x,y)\, H_0^{(2)}\left(K_m\sqrt{(x-x')^2+(y-y')^2}\right) dx'\,dy' \tag{2}$$

where $H_0^{(2)}$ is the Hankel function of order zero and of the second

Manuscript received February 17, 1982; revised May 13, 1982. This work was supported in part by DGRST, under Contract TLB-81-M0909.

The authors are with the Laboratoire Des Signaux & Systemes, Ecole Superieure D'Electricite, Plateau du Moulon, 91190 Gif-Sur-Yvette, France.

0018-9480/82/1100-1998$00.75 ©1982 IEEE